# SCIENTIFIC REPORTS

# Molecular Dynamics Simulations Reveal that Water Diffusion between Graphene Oxide Layers is Slow

Ram Devanathan, Dylan Chase-Woods, Yongsoon Shin & David W. Gotthold

Membranes made of stacked layers of graphene oxide (GO) hold the tantalizing promise of revolutionizing desalination and water filtration if selective transport of molecules can be controlled. We present the findings of an integrated study that combines experiment and molecular dynamics simulation of water intercalated between GO layers. We simulated a range of hydration levels from 1 wt.% to 23.3 wt.% water. The interlayer spacing increased upon hydration from 0.8 nm to 1.1 nm. We also synthesized GO membranes that showed an increase in layer spacing from about 0.7 nm to 0.8 nm and an increase in mass of about 15% on hydration. Water diffusion through GO layers is an order of magnitude slower than that in bulk water, because of strong hydrogen bonded interactions. Most of the water molecules are bound to OH groups even at the highest hydration level. We observed large water clusters that could span graphitic regions, oxidized regions and holes that have been experimentally observed in GO. Slow interlayer diffusion can be consistent with experimentally observed water transport in GO if holes lead to a shorter path length than previously assumed and sorption serves as a key rate-limiting step.

Graphene oxide (GO) has potential applications in opto-electronics, energy storage, solar cells, biomedical technologies, and membranes for selective molecular separation[1–6]. In particular, there is growing interest in GO membranes that allow rapid transport of water for desalination, water purification, dehumidification and filtration[7–10]. Such interest is driven by the reality that more than a billion people worldwide suffer from an acute shortage of clean water and human activity continues to pollute fresh water resources[11]. While technologies exist for waste water treatment and seawater desalination, they are inefficient, energy intensive, expensive, and environmentally unsustainable[12]. GO-based membranes hold the promise of cost-effective water filtration, because they can be rationally designed and synthesized using an inexpensive and scalable process to selectively permit certain molecules or ions to pass through.

One of the key challenges to realizing the potential of GO membranes for selective separations is the lack of mechanistic understanding of molecular interactions and transport. Even basic details, such as the structure of GO, are the subject of considerable debate and several models have been proposed to explain the structure of GO[5,13–18]. The most commonly invoked description of the chemical structure of GO is the Lerf-Klinowski model[19] and the structure is known to vary with synthesis conditions and degree of oxidation[5]. GO is considered to be amorphous and non-stoichiometric[5] with hydroxyls and epoxides as the dominant functional groups along with carbonyls at the edges of the platelets[16]. High resolution transmission electron microscopy (HRTEM) studies by Erickson $et$ $al.$[16] have revealed that the GO sheet has holes, with a typical size of 5 nm$^2$ or less, a continuous oxidized network, and isolated graphitic regions. The GO sheet is known to be rippled with surface roughness of at least 0.6 nm[13]. It is a daunting task to characterize $H_2O$ transport in GO while accounting for this heterogeneity and disorder.

Recently, the Geim group has reported[7] extraordinarily rapid permeation of $H_2O$ molecules through submicrometer thick GO membranes, which show He permeation rates that are slower than $H_2O$ permeation rates by a factor of 10$^{10}$. The authors attributed the anomalously rapid transport of $H_2O$ molecules to capillary pressure of the order of 100 MPa while a monolayer of $H_2O$ molecules flows through a network of graphene capillaries with

Pacific Northwest National Laboratory, Richland, Washington 99352, USA. Correspondence and requests for materials should be addressed to R.D. (email: ram.devanathan@pnnl.gov)

spacing between 0.6 and 1 nm. A subsequent report[8] by the same group showed that ions with hydrated radii less than 0.45 nm permeated rapidly through GO membranes by the same mechanism. A neutron scattering study by Buchsteiner et al.[20] has shown that the layer spacing of graphite oxide multilayers varies from about 0.7 to 1.1 nm with increasing humidity, the interlayer spacing and $H_2O$ uptake are affected by the synthesis method, and the spaces between layers could be filled with varying levels of water. This study also found that the interlayer $H_2O$ molecules were bound by hydrogen bonds to the oxygen of epoxide and hydroxyl groups at almost all hydration levels and bulk-like water occurred only at the highest hydration levels.

A different interpretation of $H_2O$ transport in GO membranes is provided by Talyzin et al.[21]. These authors observed the GO interlayer spacing to increase from about 0.8 to 1.2 nm following immersion in liquid water. In light of the aforementioned HRTEM studies by Erickson et al.[16] that graphene-like regions in GO are isolated, which is also evidenced by the poor electrical conductivity of GO, Talyzin et al.[21] have argued that the extraordinarily rapid water transport inferred by Nair et al.[7] is an interpretation based on an excessively long and tortuous migration path that does not account for the presence of defects and holes. Since permeation of $H_2O$ through GO will involve oxidized and unoxidized regions, Talyzin et al.[21] recommended that the flow of $H_2O$ molecules be modeled between two hydrophilic surfaces representing the structure of GO instead of two hydrophobic surfaces.

Given the experimental challenges of unambiguously characterizing water transport in the disordered environment of GO membranes, molecular modeling has a key role to play in the interpretation of experimental observations. Several molecular dynamics (MD) simulation studies have focused on water interactions with graphene[7,8,22–24]. There is a pressing need to use computer simulation to study GO-water interactions. Boukhvalov and Katsnelson[25] used density functional theory (DFT) to optimize the structure of GO and suggested the chemical formulas $C_8(OH)_2$, $C_8(OH)_2O$ and $C_8(OH)_4O$ for coverage of 25%, 50 and 75%, respectively. The spacing in a bilayer at 25% coverage was found to be 0.7 nm. A DFT study by Yan et al.[26] found that significant energy gains were attained if the OH groups formed 1,2-hydroxyl pairs on opposite sides of the GO sheet and certain combinations of epoxide and hydroxyl groups were also energetically favored. A subsequent DFT study[27] by the same group yielded optimized structures with values of bond lengths, bond angles, and displacements of oxygen atoms from the plane of graphene.

MD simulations[15,28] using reactive force fields that allow bond breaking and bond formation have shed light on hydrogen bonds between $H_2O$ molecules and functional groups in GO and the evolution of GO structure during thermal annealing. Due to the computational intensity of reactive force fields, these studies have been restricted to sample sizes of about 4 nm × 4 nm and simulation times of the order of tens of picoseconds. Wei et al.[29] performed MD simulations of $H_2O$ transport in GO with carbon atoms frozen in a planar conformation for specific interlayer distances and showed that the $H_2O$ flow is affected by electrostatic interactions in GO. Raghav et al.[30] calculated the potential of mean force for small graphene or GO sheets with 84 carbon atoms constrained as parallel layers at different separations and immersed in $H_2O$ or He, and showed that GO layers respond dynamically to their environment. Ban et al.[31] performed MD simulations of rigid $H_2O$ permeation in a rigid GO bilayer system for fixed layer separation along with experimental x-ray photoelectron spectroscopy, calorimetry and sorption measurements. The $H_2O$ diffusion coefficient in GO for layer separations greater than 1 nm calculated in this study was surprisingly higher than that in bulk $H_2O$.

In an effort to understand the molecular mechanisms that control $H_2O$ transport through GO membranes, we have performed MD simulations of model GO multilayers intercalated with $H_2O$ for different hydration levels. These simulations have provided information about bound $H_2O$, radial distribution functions, and $H_2O$ diffusion coefficients as a function of hydration level. The simulations were accompanied by experimental solution filtration and casting of GO membranes to provide information about interlayer spacing and mass increase with hydration. The present study shows that the diffusion of $H_2O$ molecules between GO layers is too slow to account for the experimentally inferred rapid transport of water through GO membranes.

## Results and Discussion

Table S1 in the Supplementary Information presents the density of the GO simulation cell at different hydration levels and it was in the range from 0.96 to 1.29 g/cm³. The layer spacing varied from 0.8 nm in GO without water to 1.1 nm in GO with intercalated water regardless of water content from 1 to 23 wt%. This change in layer spacing is consistent with the experimental results of Talyzin et al.[21] Our experimental results in Figure S1(a) show that the inter-layer spacing decreased steadily from about 0.78 nm to 0.69 nm upon vacuum drying for 9 days. On subsequent rehydration over 10 days, this spacing increased steadily from 0.69 nm to about 0.79 nm. The corresponding variation in the mass of the membrane from 10.2 mg to 8.8 mg on drying and back to 10.2 mg on rehydration can be seen in Figure S1(b). Figure S1(c) reveals that the membrane thickness decreased from 9 μm to 7 μm after drying for 9 days and increased back to 9 μm after rehydration for 10 days. The variation of the thickness gives the appearance of being non-monotonic because of the limitation of the measurement technique in that the measurements were in steps of 1 μm. Our simulation results for the layer spacing are also in good agreement with the neutron scattering results of Lerf et al.[32], who observed the layer spacing in graphite oxide to vary from 0.8 to 1.15 nm as the relative humidity (RH) increased from 45 to 100%. Experimental hydration levels are often expressed in terms of RH[20,32], while the wt.% value from our simulation is the ratio of the mass of water to the mass of water and membrane expressed as a percent. Buchsteiner et al.[20] have pointed out that RH of 75% corresponds to the uptake of a monolayer of water in the interlayer spacing. Our experimental results show that the change in mass from a fully hydrated membrane to a membrane vacuum dried for 9 days is about 15%, which can be attributed to the water removed. Even allowing for some bound water retained by the membrane during vacuum drying, the range of water content (1 to 23 wt.%) simulated in the present work covers the experimentally relevant hydration levels.

Figure 1 shows a snapshot of atom positions from simulations with 8.3 wt.% $H_2O$ and 23.3 wt.% $H_2O$. The hydroxyl groups are clustered and there are graphene-like patches between these clustered OH units. Our simple
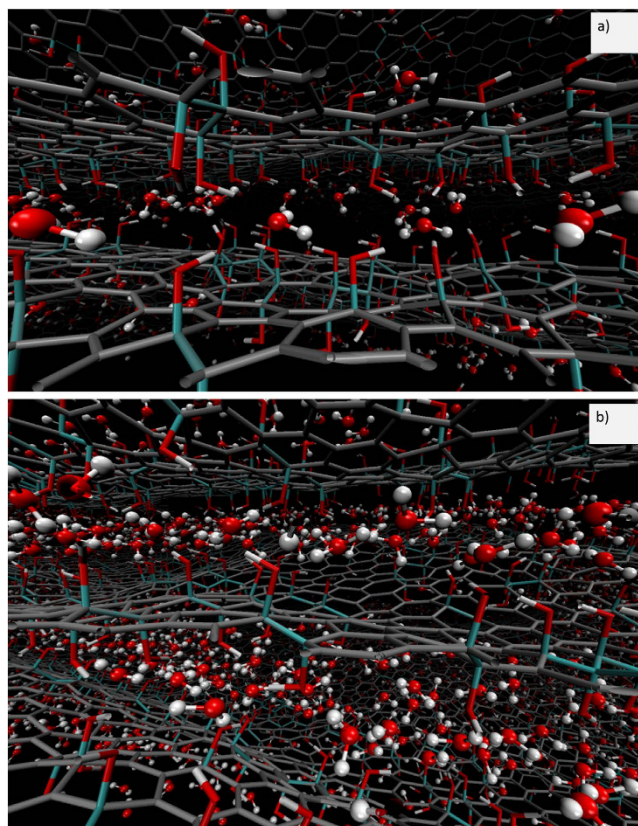
**Figure 1.** Graphene oxide configurations for (**a**) 8.3 wt.% and (**b**) 23.3 wt.% $H_2O$. O, H, C bonded to OH and other C are shown in red, white, teal and grey, respectively.

model of GO, $C_4(OH)$, has hydroxyl groups only and does not include epoxide groups or holes. The GO layers are corrugated because the atoms were not frozen and were allowed to relax. At the lower hydration level, the $H_2O$ molecules are isolated and found close to OH groups, while at the highest hydration level, clusters of $H_2O$ molecules are evident. Isolated $H_2O$ molecules are seen even more clearly at 3.9 wt.% $H_2O$ in Figure S2 of the Supplementary Information. These findings are entirely consistent with the results from reactive force field MD studies of Medhekar et al.[28] at a comparable C/O ratio—$C_{10}O_1(OH)_1$—for water content from 1 to 26 wt.%.

More evidence about water interactions in GO can be seen in the pair correlation functions between OH group oxygen ($O_h$) and water oxygen ($O_w$) and that between $O_w$ and $O_w$ presented in Fig. 2 for different hydration levels. The $O_h$-$O_w$ distribution has a sharp first peak at 0.27 nm that indicates strong binding of the $H_2O$ molecules to the OH group. With increasing hydration level, the height of this peak decreases and the longer range structure (second and subsequent peaks) starts to disappear, which shows that $H_2O$ molecules move away from the OH groups. A similar trend is seen in the $O_w$-$O_w$ pair correlation function that shows a first peak at 0.275 nm, minimum at 0.35 nm and a second peak at 0.43 nm. With increasing hydration level, the $O_w$-$O_w$ distribution approaches that of liquid water, which shows a peak value of 3.1 at 0.288 nm[33]. The inference is that $H_2O$ molecules behave more like those in bulk water as the hydration level increases. The location of the $O_h$-$O_w$ and $O_w$-$O_w$ first peaks is at a shorter separation compared to the simulation results of Medhekar et al.[28] that show an optimum O … H bond distance of 0.255 nm for two $H_2O$ molecules in GO connected by a hydrogen bond. To shed more light on hydrogen bonding in our GO-$H_2O$ system, we have calculated the pair correlation functions for the hydrogen of OH ($H_o$) and $O_w$ and for $O_h$ and the hydrogen of $H_2O$ ($H_w$). These are plotted in Figures S3 and S4, respectively, of the Supplementary Information. In both these cases, the first peak is at 0.17 nm and the first minimum is at 0.24 nm, which is completely consistent with the oxygen-oxygen distance of about 0.27 nm in our work.

Figure 3 is a plot of the percent of $H_2O$ molecules that are bound to OH groups or free (bulk-like) at various hydration levels. The details of these calculations are given in the Methods section. About 1–3% of $H_2O$ molecules do not fit into either of these categories and can be considered nearly bound. Almost all the $H_2O$ molecules are 'bound' to OH groups at the lowest hydration level of 1 wt.% $H_2O$. Our term 'bound water' includes both bound and confined water in the neutron scattering study of Buchsteiner et al.[20] while our 'free water' is similar to the 'bulk water' determined by these authors[20]. The percent of free $H_2O$ molecules increases with increasing hydration level and reaches about 21% at the highest hydration level studied. We have shown the distribution of OH groups within a distance of 0.35 nm from $H_2O$ molecules in Fig. 4(a) and the distribution of $H_2O$ molecules within a distance of 0.35 nm from OH groups in Fig. 4(b). At the highest hydration level (23.3 wt.% $H_2O$), the average $H_2O$ molecule is most likely to have one OH neighbor, while at lower hydration levels it is most likely
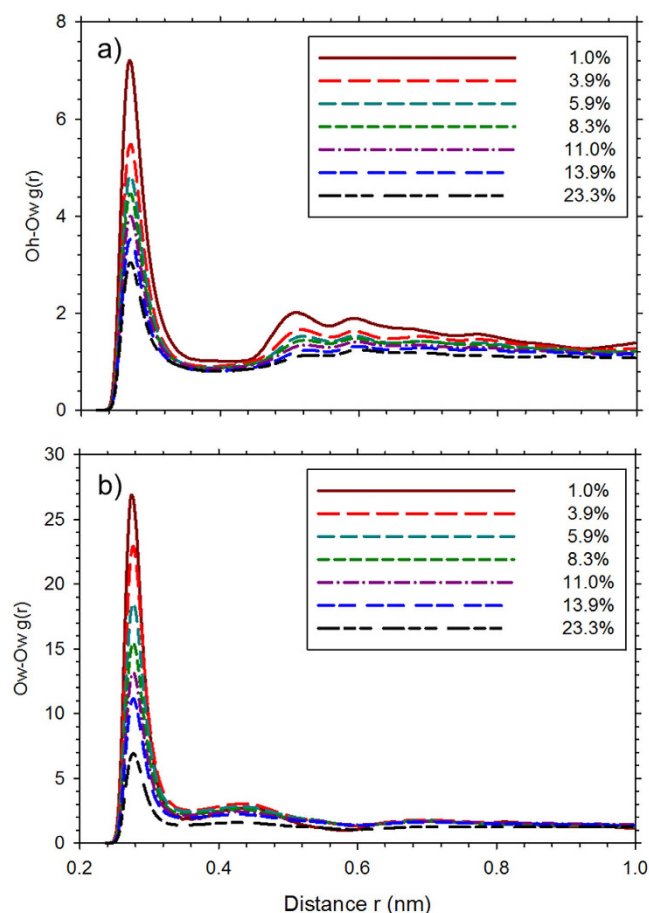
**Figure 2.** Pair correlation functions between (**a**) oxygen atoms of OH group and $H_2O$ and (**b**) oxygen atoms of $H_2O$ for the water content shown in the legend.
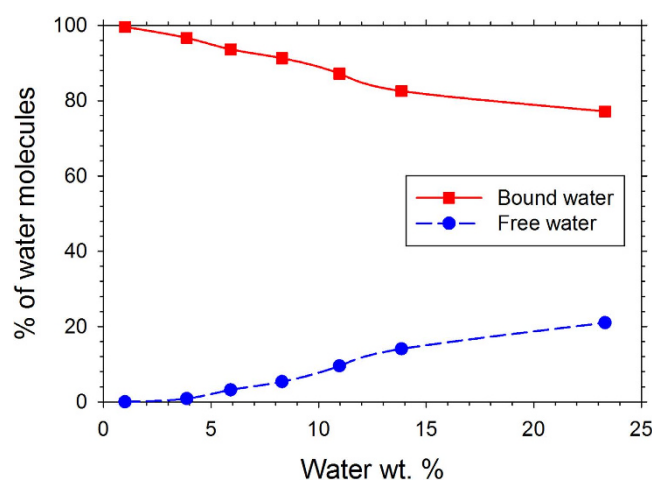


**Figure 3. Percent of bound (square) and free (circle) $H_2O$ as a function of water wt.% in graphene oxide.**

to have two OH neighbors. The model of water dynamics in graphite oxide from neutron scattering[20] includes $H_2O$ molecules hydrogen bonded to multiple functional groups. Except at the highest hydration level a large proportion of OH groups do not have $H_2O$ molecules within a distance of 0.35 nm, which is due to the fact that the number of OH groups (8230) is greater than the number of $H_2O$ molecules in those cases (see Table S1 of the Supplementary Information for details). These distributions could change if the C/O ratio is changed or if epoxide groups are introduced. Nonetheless, these findings shed light on the strong hydrogen bonding between the OH
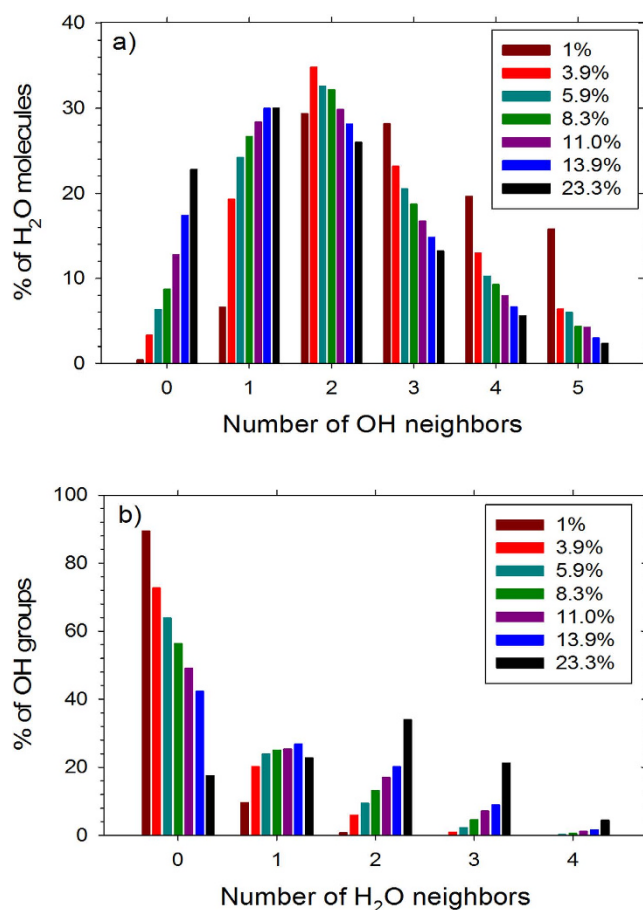
**Figure 4.** (**a**) Distribution of OH groups near $H_2O$ molecules and (**b**) distribution of $H_2O$ molecules near OH groups based on a cutoff distance of 0.35 nm between $O_h$ and $O_w$.
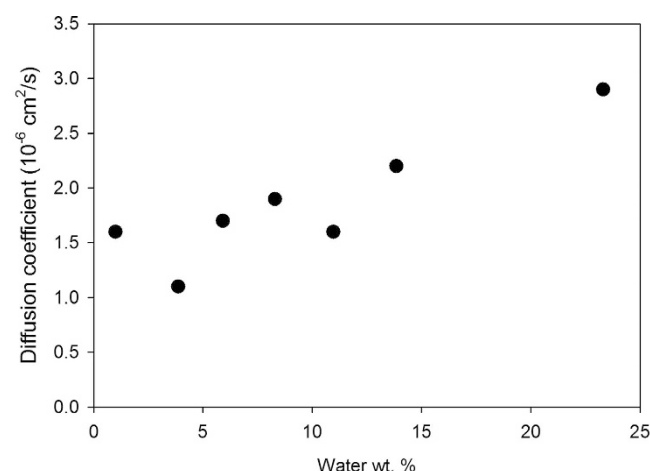


**Figure 5. The diffusion coefficient of water as a function of hydration level in graphene oxide.**

groups and $H_2O$ molecules. Our results are in good agreement with the finding of the neutron scattering study of water in graphite oxide[20] that water is tightly bound except at the highest humidity level studied.

The effect of hydration level on the water diffusion coefficient ($D_w$) in GO is presented in Fig. 5. $D_w$ shows a general increasing trend with increasing hydration level although there is some scatter in the data. These values are an order of magnitude less than the diffusion coefficient in bulk water, which is to be expected given the strong hydrogen bonded interaction with OH groups at all hydration levels. Diffusion at the lowest hydration level, where almost all $H_2O$ molecules are bound, could still occur by migration between adjacent OH groups as suggested by Buchsteiner *et al.*[20] based on neutron scattering.

As the water content increases, the percent of water molecules that are free increases substantially from about 3.2% at a hydration level of 5.9 wt.% water to 21% at 23.3 wt.% water. This increase results in faster diffusion, because a larger proportion of water molecules can move unhindered by OH groups. The average water cluster size increases with hydration level as shown in Figure S5 of the Supplementary information. If isolated water molecules (cluster size $n = 1$ molecule) are included, the average cluster size increases from 1.2 molecules for a hydration level of 1 wt.% water to 33.7 molecules for 23.3 wt.% water. If isolated molecules are excluded from the definition of a cluster, these numbers are 2.3 and 83.2 molecules, respectively. The largest $H_2O$ cluster size varied from 10 molecules at 1 wt.% water to 2948 molecules at 23.3 wt.% as shown in Table S2 of the Supplementary Information. Some of these clusters are large enough to extend from the oxidized region to the unoxidized regions or holes that have been experimentally observed.

The present simulations show strong hydrogen bonding between OH groups and $H_2O$ molecules resulting in slow water diffusion in GO, which has important implications for the recent interpretation by the Geim group[7] that $H_2O$ molecules are transported at an extraordinarily rapid rate through GO membranes by graphene capillaries. Since it has been experimentally shown[16] that graphitic regions in GO layers are isolated while the oxidized regions are continuous, fast transport through graphitic regions cannot entirely explain the observed rapid water permeation. Recently, Huang et al.[34] examined the separation performance of GO for dimethyl carbonate (DMC)/water and methanol/water mixtures and the sorption of DMC, methanol and water on GO. They concluded that preferential transport of molecules through GO is influenced by both sorption and interlayer diffusion. In a subsequent study by the same group[35], the water transport and selective separation of water from n-butanol was found to be enhanced when a hydrophilic polymer layer was deposited on the surface of GO laminates. Rapid water permeation was attributed to increased water sorption due to the hydrophilic surface and the availability of molecular channels within the GO laminates. A recent review of GO membranes[36] has pointed that interlayer channels, defects or holes, and functional groups are important factors controlling molecular transport through GO.

Large water clusters, observed in the present work, could bridge graphitic and oxidized regions as well as holes. The graphitic regions could be isolated or extensive depending on the C/O ratio and the synthesis method. Rapid interlayer water transport is unlikely through the GO region, but could take place through a shorter path between graphitic regions via holes and spaces between flakes. The functional groups lining the holes and the hydrogen bonded network in the oxidized regions seen in the present study will hinder the transport of solvated ions and thus contribute to the observed selective transport. Further simulation of molecular sorption at the GO surface and transport of molecules and ions through GO containing holes and representative graphitic regions is needed to shed more light on selective transport in GO, especially for desalination.

## Conclusions

We have performed molecular dynamics simulations of water interactions in graphene oxide (GO) membrane at several hydration levels. We considered a model system with hydroxyl groups only and a C/O ratio of 4. Our results show that water diffusion in GO is an order of magnitude slower than in bulk water due to strong hydrogen bonded interactions between $H_2O$ molecules and the OH group. The optimum distance for the hydrogen bond (O··H) in our simulation is 0.17 nm and the oxygen-oxygen distance is typically 0.27 nm. Even at the highest hydration level of 23.3 wt.% $H_2O$, only about 21% of the $H_2O$ molecules were free or bulk-like. We observed large water clusters comprising 10 to 30% of the water molecules present in the system. Such clusters can span across oxidized regions, graphitic regions, and defects or holes that have been seen in experiments thereby contributing to rapid water transport. Our results are in good agreement with results from neutron scattering studies of hydrated GO layers.

## Methods

We synthesized membranes from a range of different GO sources, both commercial and prepared at Pacific Northwest National Laboratory (PNNL), with the goal of obtaining various flake sizes, from 100 nm to 100 μm in nominal diameter. We used a simple solution filtration and casting on a polytetrafluoroethylene plate (12" × 12") to isolate free-standing GO membranes. In addition to the variable flake sizes, we prepared membranes with thicknesses ranging from 5 μm to 50 μm and characterized them using multiple measurement techniques including X-ray diffraction pattern to detect the change in layer spacing that accompanies changes in mass and thickness of GO with changes in the hydration level.

We performed classical molecular dynamics simulations of GO membranes with $H_2O$ using the DLPOLY4 computer code[37]. We chose the composition $C_8(OH)_2$ suggested by Boukhvalov and Katsnelson[25] and obtained the charges of the hydroxyl group from a restricted electrostatic potential fit following calculations at the B3LYP/6-31G* level of theory[38,39] using the Gaussian 98 program[40]. The charges of O, H, and C bonded to the OH group in the present simulation are −0.53$e$, 0.35$e$ and 0.18$e$, respectively, where $e$ is the magnitude of the electron charge. All other carbon atoms are uncharged. We used the DREIDING[41] force field to describe the GO layer, the F3C[42] potential for $H_2O$, and the non-bonded interaction parameters of Wu and Aluru[43] for the C-$H_2O$ interactions. We used harmonic bond stretching and angle bending terms with bond lengths and bond angles constrained to correspond to the relaxed GO structure calculated by Yan and Chou[27].

The simulation cell contained three layers of GO and was periodically repeated in all dimensions. We created GO layers with a C/O ratio of about 4 by randomly selecting two adjacent C atoms that were not already bonded to hydroxyl groups and attaching 1,2-hydroxyl pairs on opposite sides of the layer in a configuration optimized by Yan et al.[26]. The distribution of OH groups is different for each layer, and the three layers together had 33120 C atoms and 8230 OH groups. Starting with a layer spacing of 1.5 nm, we introduced a monolayer of $H_2O$ molecules between the GO layers with the number of $H_2O$ molecules ranging from 300 to 9075. We studied eight different hydration levels with water weight% varying from 0 to 23.9%. These values cover the range of $H_2O$ content seen

in our experimental samples and presented in Figure S6 of the Supplementary Information. The GO-$H_2O$ system was annealed for 4 ns in the temperature range from 300 to 600 K as described previously[44]. We did not freeze any atom, fix the layer separation, fix the density of the system, or constrain the distribution of water molecules. After equilibration, the size of the simulation cell was about 17 nm × 17 nm × 3 nm.

We carried out the production run at constant volume and temperature of 300 K for 5 ns with a time step of 1 fs. We determined the $H_2O$ diffusion coefficient from the last 1 ns of data by performing a linear regression to the mean square displacement vs. time. We calculated the radial distribution functions for different pairs of atoms and obtained the number of bound $H_2O$ molecules by considering a molecule to be bound if the distance between water oxygen ($O_w$) and OH group oxygen ($O_h$) was less than 0.35 nm. A $H_2O$ molecule was considered to be free if that $O_w$ was surrounded by four or more $O_w$ within a distance of 0.4 nm. We also determined the extent of clustering of $H_2O$ molecules by considering two molecules to belong to the same cluster if the $O_w$-$O_w$ separation was less than 0.35 nm as discussed previously[44–46].

## References

1. Dikin, D. A. *et al.* Preparation and characterization of graphene oxide paper. *Nature* **448,** 457–460 (2007).
2. Eda, G., Fanchini, G. & Chhowalla, M. Large-area ultrathin films of reduced graphene oxide as a transparent and flexible electronic material. *Nature nanotechnology* **3,** 270–274 (2008).
3. Park, S. & Ruoff, R. S. Chemical methods for the production of graphenes. *Nature nanotechnology* **4,** 217–224 (2009).
4. Loh, K. P., Bao, Q., Eda, G. & Chhowalla, M. Graphene oxide as a chemically tunable platform for optical applications. *Nat Chem* **2,** 1015–1024 (2010).
5. Dreyer, D. R., Park, S., Bielawski, C. W. & Ruoff, R. S. The chemistry of graphene oxide. *Chemical Society Reviews* **39,** 228–240 (2010).
6. Hu, M. & Mi, B. Enabling Graphene Oxide Nanosheets as Water Separation Membranes. *Environmental Science & Technology* **47,** 3715–3723, doi: 10.1021/es400571g (2013).
7. Nair, R. R., Wu, H. A., Jayaram, P. N., Grigorieva, I. V. & Geim, A. K. Unimpeded Permeation of Water Through Helium-Leak–Tight Graphene-Based Membranes. *Science* **335,** 442–444, doi: 10.1126/science.1211694 (2012).
8. Joshi, R. K. *et al.* Precise and Ultrafast Molecular Sieving Through Graphene Oxide Membranes. *Science* **343,** 752–754, doi: 10.1126/science.1245711 (2014).
9. Mi, B. Graphene Oxide Membranes for Ionic and Molecular Sieving. *Science* **343,** 740–742, doi: 10.1126/science.1250247 (2014).
10. Joshi, R. K., Alwarappan, S., Yoshimura, M., Sahajwalla, V. & Nishina, Y. Graphene oxide: the new membrane material. *Applied Materials Today* **1,** 1–12, doi: http://dx.doi.org/10.1016/j.apmt.2015.06.002 (2015).
11. Shannon, M. A. *et al.* Science and technology for water purification in the coming decades. *Nature* **452,** 301–310 (2008).
12. Elimelech, M. & Phillip, W. A. The Future of Seawater Desalination: Energy, Technology, and the Environment. *Science* **333,** 712–717, doi: 10.1126/science.1200488 (2011).
13. Mkhoyan, K. A. *et al.* Atomic and electronic structure of graphene-oxide. *Nano letters* **9,** 1058–1063 (2009).
14. Gao, W., Alemany, L. B., Ci, L. & Ajayan, P. M. New insights into the structure and reduction of graphite oxide. *Nat Chem* **1,** 403–408, doi: http://www.nature.com/nchem/journal/v1/n5/suppinfo/nchem.281_S1.html (2009).
15. Bagri, A. *et al.* Structural evolution during the reduction of chemically derived graphene oxide. *Nature chemistry* **2,** 581–587 (2010).
16. Erickson, K. *et al.* Determination of the local chemical structure of graphene oxide and reduced graphene oxide. *Advanced Materials* **22,** 4467–4472 (2010).
17. Dimiev, A., Kosynkin, D. V., Alemany, L. B., Chaguine, P. & Tour, J. M. Pristine Graphite Oxide. *Journal of the American Chemical Society* **134,** 2815–2822, doi: 10.1021/ja211531y (2012).
18. Dimiev, A. M., Alemany, L. B. & Tour, J. M. Graphene oxide. Origin of acidity, its instability in water, and a new dynamic structural model. *ACS nano* **7,** 576–588 (2012).
19. Lerf, A., He, H. Y., Forster, M. & Klinowski, J. Structure of graphite oxide revisited. *J. Phys. Chem. B* **102,** 4477–4482, doi: 10.1021/jp9731821 (1998).
20. Buchsteiner, A., Lerf, A. & Pieper, J. Water Dynamics in Graphite Oxide Investigated with Neutron Scattering. *The Journal of Physical Chemistry B* **110,** 22328–22338, doi: 10.1021/jp0641132 (2006).
21. Talyzin, A. V., Hausmaninger, T., You, S. & Szabó, T. The structure of graphene oxide membranes in liquid water, ethanol and water–ethanol mixtures. *Nanoscale* **6,** 272–281 (2014).
22. Ma, J. *et al.* Adsorption and diffusion of water on graphene from first principles. *Physical Review B* **84,** 033402 (2011).
23. Cohen-Tanugi, D. & Grossman, J. C. Water desalination across nanoporous graphene. *Nano letters* **12,** 3602–3608 (2012).
24. Konatham, D., Yu, J., Ho, T. A. & Striolo, A. Simulation insights for graphene-based water desalination membranes. *Langmuir* **29,** 11884–11897 (2013).
25. Boukhvalov, D. W. & Katsnelson, M. I. Modeling of graphite oxide. *Journal of the American Chemical Society* **130,** 10697–10701 (2008).
26. Yan, J.-A., Xian, L. & Chou, M. Structural and electronic properties of oxidized graphene. *Physical review letters* **103,** 086802 (2009).
27. Yan, J.-A. & Chou, M. Oxidation functional groups on graphene: Structural and electronic properties. *Physical review B* **82,** 125403 (2010).
28. Medhekar, N. V., Ramasubramaniam, A., Ruoff, R. S. & Shenoy, V. B. Hydrogen bond networks in graphene oxide composite paper: structure and mechanical properties. *Acs Nano* **4,** 2300–2306 (2010).
29. Wei, N., Peng, X. & Xu, Z. Breakdown of fast water transport in graphene oxides. *Physical Review E* **89,** 012113 (2014).
30. Raghav, N., Chakraborty, S. & Maiti, P. K. Molecular mechanism of water permeation in a helium impermeable graphene and graphene oxide membrane. *Physical Chemistry Chemical Physics* **17,** 20557–20562 (2015).
31. Ban, S. *et al.* Insight into the nanoscale mechanism of rapid $H_2O$ transport within graphene oxide membrane: the impact of oxygen functional group clustering. *ACS applied materials & interfaces* (2015).
32. Lerf, A. *et al.* Hydration behavior and dynamics of water molecules in graphite oxide. *Journal of Physics and Chemistry of Solids* **67,** 1106–1110 (2006).
33. Soper, A. & Phillips, M. A new determination of the structure of water at 25 C. *Chemical Physics* **107,** 47–60 (1986).
34. Huang, K. *et al.* A graphene oxide membrane with highly selective molecular separation of aqueous organic solution. *Angewandte Chemie International Edition* **53,** 6929–6932 (2014).
35. Huang, K. *et al.* High-Efficiency Water-Transport Channels using the Synergistic Effect of a Hydrophilic Polymer and Graphene Oxide Laminates. *Advanced Functional Materials* **25,** 5809–5815 (2015).
36. Liu, G., Jin, W. & Xu, N. Graphene-based membranes. *Chemical Society Reviews* **44,** 5016–5030 (2015).
37. Todorov, I. T., Smith, W., Trachenko, K. & Dove, M. T. DL_POLY_3: new dimensions in molecular dynamics simulations via massive parallelism. *Journal of Materials Chemistry* **16,** 1911–1918 (2006).
38. Becke, A. D. Density-functional thermochemistry. III. The role of exact exchange. *The Journal of chemical physics* **98,** 5648–5652 (1993).

39. Hehre, W. J., Ditchfield, R. & Pople, J. A. Self—consistent molecular orbital methods. XII. Further extensions of Gaussian—type basis sets for use in molecular orbital studies of organic molecules. *The Journal of Chemical Physics* **56,** 2257–2261 (1972).
40. Frisch, M. *et al.* Gaussian 98, revision a. 7; gaussian. *Inc., Pittsburgh, PA* **12** (1998).
41. Mayo, S. L., Olafson, B. D. & Goddard, W. A. DREIDING: a generic force field for molecular simulations. *Journal of Physical Chemistry* **94,** 8897–8909 (1990).
42. Levitt, M., Hirshberg, M., Sharon, R., Laidig, K. E. & Daggett, V. Calibration and testing of a water model for simulation of the molecular dynamics of proteins and nucleic acids in solution. *The Journal of Physical Chemistry B* **101,** 5051–5061 (1997).
43. Wu, Y. & Aluru, N. R. Graphitic Carbon–Water Nonbonded Interaction Parameters. *The Journal of Physical Chemistry B* **117,** 8802–8813, doi: 10.1021/jp402051t (2013).
44. Devanathan, R., Venkatnathan, A. & Dupuis, M. Atomistic simulation of nafion membrane: I. effect of hydration on membrane nanostructure. *The Journal of Physical Chemistry B* **111,** 8069–8079 (2007).
45. Devanathan, R., Venkatnathan, A. & Dupuis, M. Atomistic simulation of Nafion membrane. 2. Dynamics of water molecules and hydronium ions. *The Journal of Physical Chemistry B* **111,** 13006–13013 (2007).
46. Devanathan, R. *et al.* Atomistic simulation of water percolation and proton hopping in nafion fuel cell membrane. *The Journal of Physical Chemistry B* **114,** 13681–13690 (2010).

## Acknowledgements

## Author Contributions

R.D. performed the simulations, analyzed the data and prepared the manuscript. D.C.-W. assisted with the analysis of the data. Y.S. synthesized the GO membranes and determined the interlayer spacing. Y.S. and D.W.G. provided experimental insights to interpret the simulation results. All authors reviewed the manuscript.

## Additional Information

**Supplementary information** accompanies this paper at http://www.nature.com/srep

**Competing financial interests:** The authors declare no competing financial interests.

**How to cite this article**: Devanathan, R. *et al.* Molecular Dynamics Simulations Reveal that Water Diffusion between Graphene Oxide Layers is Slow. *Sci. Rep.* **6**, 29484; doi: 10.1038/srep29484 (2016).